Synthesis and Characterization of Bimagnetic Bricklike Nanoparticles

Girija S. Chaubey, Vikas Nandwana, Narayan Poudyal, Chuan-bing Rong, and J. Ping Liu*

Department of Physics, University of Texas at Arlington, Arlington, Texas 76019

Received September 28, 2007. Revised Manuscript Received November 8, 2007

Bimagnetic FePt/$CoFe_2O_4$ nanoparticles having a bricklike morphology were synthesized by growing a soft magnetic $CoFe_2O_4$ phase on FePt cubic nanoparticle seeds. The size of the soft phase could be controlled by tuning the material ratio of the FePt seeds to the $CoFe_2O_4$ component. To obtain magnetic hardening, the as-synthesized bricklike nanoparticles were annealed at elevated temperatures under a reductive atmosphere to convert the disordered face-centered cubic FePt phase into the ordered $L1_0$ phase having high magnetic anisotropy. When the particles were annealed, a gradual change was observed in morphology from bricklike particles to spherical polycrystalline nanocomposite particles because of diffusion. Meanwhile, the magnetic energy density was enhanced as a result of the exchange coupling between the hard and soft phases. The enhancement was dependent on the ratio of the volumes of the soft phase and the hard phase.

Introduction

The major interest in recent materials research lies not only in synthesizing new materials but also in controlling the morphology of materials to produce desired nanostructures, for instance, nanoparticles with controllable sizes and shapes. The developments in nanoparticle synthesis from single-component nanoparticles to nanoparticles with two or more components are attractive for advanced applications. For instance, core/shell-structured semiconductor nanoparticles with wide-band-gap shells over narrow-band-gap cores have higher luminescence quantum yields than single-component semiconductor nanocrystalline materials.[1–3] For biological applications, nanoparticles with a magnetic material encapsulated in a nonmagnetic material or a nonmagnetic material encapsulated in a magnetic material are interesting.[4–6] Bimagnetic nanoparticles consisting of a hard magnetic phase and a soft magnetic phase have high potential applications in magnetic recording media[7–9] and permanent magnetic materials[10–12] because the intimate contact between the hard and soft magnetic phases in the nanoparticles enhances interphase exchange coupling. Most of the bimagnetic nanoparticle systems reported to date have core/shell structures in which the core components are covered completely by the shells.

In this paper, we report the synthesis and characterization of bimagnetic nanoparticles having a novel morphology: bricklike nanoparticles, which consist of two components, FePt and $CoFe_2O_4$ (with the oxide phase attached to the FePt phase), forming shadow images of each other. Unlike a magnetic hard-core/soft-shell structure, the thickness of both components can be tuned to a large extent. This makes it easy to control the ratio of the two components and thus to adjust the magnetic properties.

Experimental Procedures

All of the reagents used in this synthesis were commercially available and used as received without further purification. Iron(III) acetylacetonate [$Fe(acac)_3$], cobalt(II) acetylacetonate [$Co(acac)_2$], iron pentacarbonyl [$Fe(CO)_5$], 1,2-hexadecanediol, oleylamine, and oleic acid were purchased from Sigma-Aldrich. Platinum(II) acetylacetonate [$Pt(acac)_2$] was obtained from Strem Chemical. All of the reactions were carried out using standard Schlenk-line technique.

Synthesis of FePt Nanoparticles. The 8 nm cubic FePt particles were synthesized by chemical reduction of $Pt(acac)_2$ and thermal decomposition of $Fe(CO)_5$ in the presence of surfactants, as reported previously.[13] In brief, 0.5 mmol of platinum acetylacetonate was added to a 125 mL flask containing a magnetic stir bar and mixed with 20 mL of octyl ether. The flask was purged with argon for 30 min at room temperature and then heated to 120 °C for 10 min, after which designated amounts of oleic acid and oleylamine were

* Email: pliu@uta.edu.

(1) Kortan, A. R.; Hull, R.; Opila, R. L.; Bawendi, M. G.; Steigerwald, M. L.; Carrol, P. J.; Brus, L. E. *J. Am. Chem. Soc.* **1990**, *112*, 1327–1332.
(2) Dabbousi, B. O.; Rodriguez-Viejo, J.; Mikulec, F. V.; Heine, J. R.; Mattoussi, H.; Ober, R.; Jensen, K. F.; Bawendi, M. G. *J. Phys. Chem. B* **1997**, *101*, 9463–9475.
(3) Reiss, P.; Bleuse, J.; Pron, A. *Nano Lett.* **2002**, *2*, 781–784.
(4) Shi, W.; Sahoo, Y.; Zeng, H.; Ding, Y.; Swihart, M. T.; Prasad, P. N. *Adv. Mater.* **2006**, *18*, 1889–1894.
(5) Cho, S.; Shahin, A. M.; Long, G. J.; Davies, J. E.; Liu, K.; Grandjean, F.; Kauzlarich, S. M. *Chem. Mater.* **2006**, *18*, 960–967.
(6) Shi, W.; Zeng, H.; Sahoo, Y.; Ohulchanskyy, T. Y.; Ding, Y.; Wand, Z. L.; Swihart, M. T.; Prasad, P. N. *Nano Lett.* **2006**, *6*, 875–881.
(7) Wang, J. P.; Shen, W.; Bai, J. *IEEE Trans. Magn.* **2005**, *41*, 3181–3186.
(8) Victora, R. H.; Shen, X. *IEEE Trans. Magn.* **2005**, *41*, 2828–2833.
(9) Suess, D.; Schrefl, T.; Fähler, F.; Kirschner, M.; Hrkac, G.; Dorfbauer, F.; Fidler, J. *Appl. Phys. Lett.* **2005**, *87*, 012504-1–012504-3.
(10) Zeng, H.; Li, J.; Liu, J. P.; Wang, Z. L.; Sun, S. *Nature* **2002**, *420*, 395–398.
(11) Zeng, H.; Sun, S.; Li, J.; Wang, Z. L.; Liu, J. P. *Appl. Phys. Lett.* **2004**, *85*, 792–794.
(12) Zeng, H.; Li, J.; Wang, Z. L.; Liu, J. P.; Sun, S. *Nano Lett.* **2004**, *4*, 187–190.
(13) Nandwana, V.; Elkins, K. E.; Poudyal, N.; Chaubey, G. S.; Yano, K.; Liu, J. P. *J. Phys. Chem. C* **2007**, *111*, 4185–4189.

10.1021/cm7028068 CCC: $40.75
Published on Web 12/22/2007

added. Iron pentacarbonyl (1.0 mmol) was added at 120 °C when the platinum precursor had dissolved completely. The dissolution of $Pt(acac)_2$ in the solvent was followed experimentally by the change of color of the solution from off-yellow to transparent yellow. After the addition of $Fe(CO)_5$, the color transition from golden to black suggested formation of nanoparticles in the solution, at which point the solution was heated to 298 °C for 1 h and then cooled to room temperature under an argon blanket. A flow of argon gas was maintained throughout the experiment. The black product was precipitated by addition of ethanol, separated by centrifugation, and redispersed in hexane.

Synthesis of FePt/$CoFe_2O_4$ Bricklike Nanoparticles. As-synthesized 8 nm FePt nanoparticles serving as seeds were mixed with $Co(acac)_2$ and $Fe(acac)_3$ in phenyl ether in the presence of 1,2-hexadecanediol, oleic acid, and oleylamine. Bricklike FePt/$CoFe_2O_4$ nanoparticles were obtained by refluxing the reaction mixture at 265 °C for 30 min.[14] Bimagnetic bricklike FePt/$CoFe_2O_4$ nanoparticles were isolated by centrifugation. The size of the soft phase could be controlled by varying the material ratio of FePt nanoparticle seeds to $CoFe_2O_4$ metal precursors. A typical procedure for obtaining FePt/$CoFe_2O_4$ bricklike nanoparticles having 8 nm FePt and 8 nm $CoFe_2O_4$ was the following:

$Co(acac)_2$ (0.05 mmol), $Fe(acac)_3$ (0.1 mmol), 1,2-hexadecanediol (10 mmol), oleic acid (10 mmol), and oleylamine (10 mmol) were mixed in 20 mL of phenyl ether and magnetically stirred under an argon atmosphere, and 90 mg of 8 nm FePt seeds (dry powder) was added to the reaction mixture. After the mixture was purged with argon for 30 min at room temperature, it was heated to 100 °C for 20 min and then to 200 °C for 60 min, refluxed at 265 °C for 30 min, and finally cooled to room temperature. The black product was precipitated by addition of 20 mL of ethanol and separated via centrifugation. The product was washed two or three times using a mixture of hexane (10 mL) and ethanol (40 mL) and separated via centrifugation. Finally, the product, 8 nm FePt/8 nm $CoFe_2O_4$ bricklike nanoparticles, was redispersed in hexane.

Annealing Procedure. The hexane dispersion of the bricklike nanoparticles was dropped onto a carbon-coated copper grid for use in transmission electron microscopy (TEM). The copper grid was placed in an alumina boat on a silica substrate. The boat was then placed in a heating furnace and purged with a gas mixture (93% Ar + 7% H_2) for 20 min. The samples were heated to the desired annealing temperatures under a continuous flow of the gas mixture.

The morphology of the nanoparticles was observed using TEM. Samples for TEM analysis were prepared by drying a hexane dispersion of the particles on amorphous carbon-coated copper grids. X-ray diffraction (XRD) patterns of the particle assemblies were collected on a diffractometer with Cu Kα radiation ($\lambda = 1.5406$ Å). Magnetic measurements were carried out using a superconducting quantum interference device (SQUID) magnetometer. Composition analysis was done using energy-dispersive X-ray spectroscopy (EDX) and inductively coupled plasma analysis (ICP).

Results and Discussion

Figure 1A shows a TEM image of as-synthesized FePt particles having an average diameter of 8 nm that were used as seeds. Most of the particles were of cuboidal shape. The composition of the particles was determined by EDX and ICP and found to be $Fe_{46}Pt_{54}$. Figure 1B,C shows typical TEM images of bricklike FePt/$CoFe_2O_4$ nanoparticles with

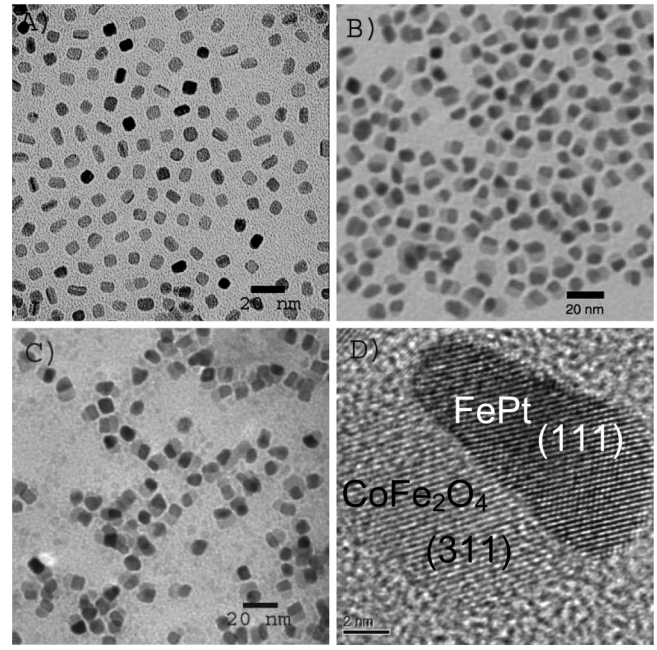

Figure 1. TEM images of as-synthesized nanoparticles: (A) 8 nm FePt; (B) 8 nm/8 nm FePt/$CoFe_2O_4$; (C) 8 nm/10 nm FePt/$CoFe_2O_4$; (D) HRTEM of as-synthesized 8 nm/8 nm FePt/$CoFe_2O_4$.

side attachment, in which the components form shadow images of each other. Each 8 nm average size FePt particle (darker contrast) is attached to a $CoFe_2O_4$ particle (lighter contrast) having an average size of 8 nm (Figure 1B) or 10 nm (Figure 1C). As-synthesized FePt/$CoFe_2O_4$ bricklike particles were further characterized by high-resolution transmission electron microscopy (HRTEM), as shown in Figure 1D. It is clearly seen that both components are single-crystalline. The HRTEM analysis of the as-synthesized bricklike nanoparticles revealed that the structure of the darker-contrast region of each bricklike nanoparticle was chemically disordered face-centered cubic (fcc) FePt while the lighter-contrast region was $CoFe_2O_4$. Detailed HRTEM analysis of several as-synthesized bricklike particles further revealed that the (111) plane of the fcc FePt phase attaches to the (311) plane of the $CoFe_2O_4$ phase. Using cubic FePt nanoparticle seeds was the key point in obtaining homogeneous bricklike FePt/$CoFe_2O_4$ nanoparticles. Nevertheless, bimagnetic FePt/$CoFe_2O_4$ nanoparticles could be obtained even when spherical FePt particles were used as seeds. However, in that case, the volume of $CoFe_2O_4$ attached to each FePt particle was not the same as that of the cubic nanoparticles, and the morphology was also different from that of the bricklike particles. It is to be noted that bricklike FePt/$CoFe_2O_4$ nanoparticles were obtained when the reaction mixture was refluxed for 30 min at 265 °C. When the refluxing time was increased from 30 min to 2 h, FePt/$CoFe_2O_4$ core/shell nanoparticles were obtained under the similar reaction conditions; this may be attributed to sphericization of the cubic seed particles during the long refluxing process. Figure 2 shows XRD patterns of the as-synthesized 8 nm FePt assembly (Figure 2A), the as-synthesized 8 nm $CoFe_2O_4$ particles (Figure 2B), and the FePt/$CoFe_2O_4$ bricklike nanoparticles (Figure 2C). A comparison of Figure 2A,B

(14) Sun, S.; Zeng, H.; Robinson, D. B.; Raoux, S.; Rice, P. M.; Wang, S. X.; Li, G. *J. Am. Chem. Soc.* **2004**, *126*, 273–279.

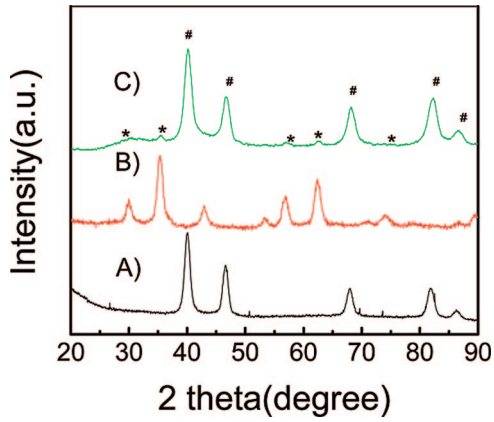

Figure 2. XRD patterns of as-synthesized nanoparticles: (A) 8 nm FePt; (B) 8 nm $CoFe_2O_4$; (C) 8 nm/8 nm FePt/$CoFe_2O_4$ (* and # indicate $CoFe_2O_4$ and FePt peaks, respectively).

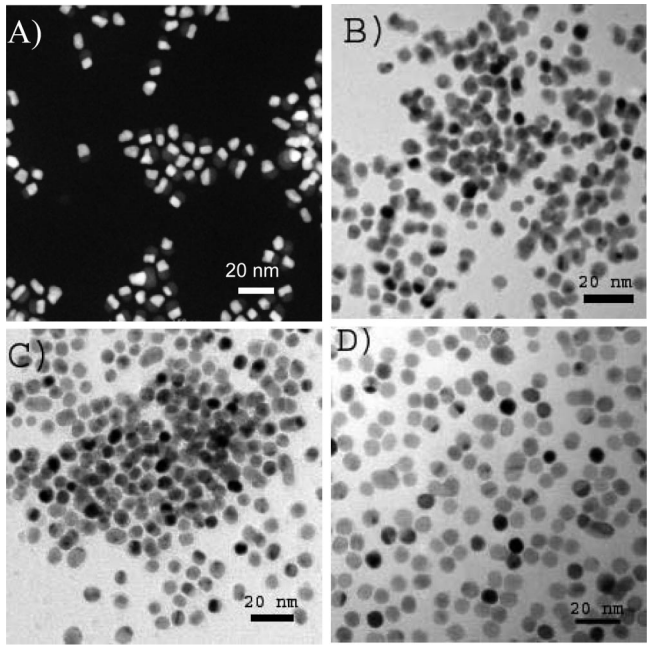

Figure 3. (A) Dark-field TEM image of an assembly of 8 nm/8 nm FePt/$CoFe_2O_4$ bricklike nanoparticles annealed for 3 h at 400 °C. Bright-field TEM images of assemblies of 8 nm/8 nm FePt/$CoFe_2O_4$ bricklike nanoparticles annealed for 2 h at (B) 500 °C, (C) 600 °C, and (D) 700 °C. All annealing was performed under a reductive gas mixture (93% Ar + 7% H_2).

with Figure 2C clearly shows that Figure 2C contains two sets of peaks, one set corresponding to the chemically disordered fcc FePt phase and the other set to the $CoFe_2O_4$ phase. The low intensity of the $CoFe_2O_4$ peaks in Figure 2C could be due to the difference in absorption coefficients of the two materials.[15]

The chemically disordered fcc FePt crystals had a low magnetocrystalline anisotropy. To obtain magnetic hardening, the as-synthesized FePt/$CoFe_2O_4$ bricklike nanoparticles were annealed at increasing temperatures under a reductive atmosphere (93% Ar + 7% H_2). Figures 3 and 4 show TEM images and XRD patterns, respectively, of FePt/$CoFe_2O_4$ bricklike nanoparticles annealed at various temperatures. It

(15) Cullity, B. D. *Elements of X-ray Diffraction*; Addison-Wesley: Reading, MA, 1959.

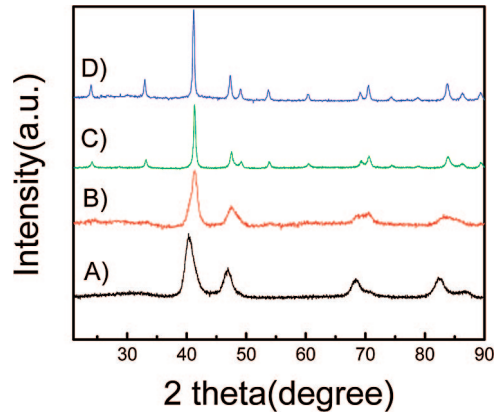

Figure 4. XRD patterns of 8 nm/8 nm FePt/$CoFe_2O_4$ bricklike nanoparticles annealed under a reductive gas mixture (93% Ar + 7% H_2) at (A) 400 °C for 3 h, (B) 500 °C for 2 h, (C) 600 °C for 2 h, and (D) 700 °C for 2 h.

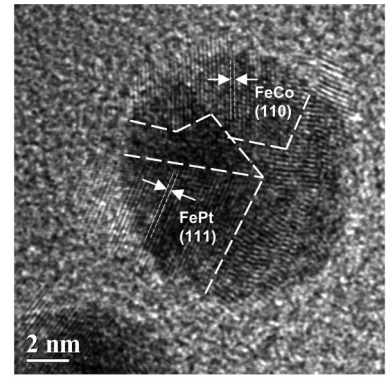

(A)

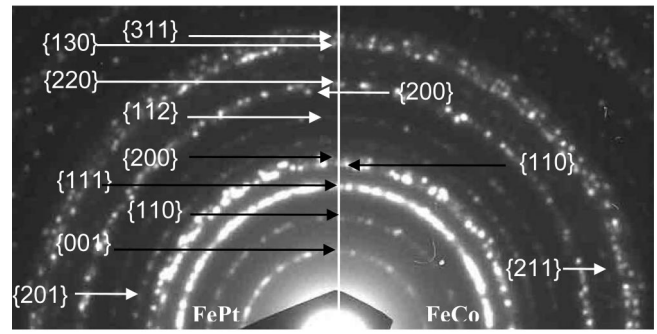

(B)

Figure 5. (A) HRTEM image of a single FePt/$CoFe_2O_4$ bricklike nanoparticle annealed at 700 °C under a reductive gas mixture (93% Ar + 7% H_2). (B) SAED pattern of a FePt/$CoFe_2O_4$ bricklike particle annealed at 700 °C under a reductive gas mixture (93% Ar + 7% H_2).

can be seen clearly that annealing of the FePt/$CoFe_2O_4$ bricklike particles at 400 °C for 3 h did not result in any morphology change. The XRD pattern of the sample annealed at 400 °C (Figure 4A) does not show any peak for the oxide, indicating that the oxide was reduced while the FePt component retained its fcc structure. The bricklike particles were further annealed at 500 °C. While a few of the particles still retained a partial brick shape, the bricklike morphology of most of the particles disappeared after annealing at 500 °C as a result of restructuring (Figure 3B). XRD analysis of the sample annealed at 500 °C showed that the phase transformation of FePt from chemically disordered

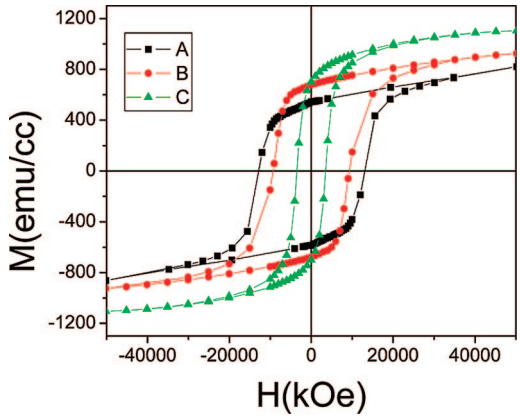

Figure 6. Room-temperature hysteresis loops of (A) 8 nm FePt nanoparticle seeds, (B) an annealed assembly of 8 nm/8 nm $FePt/CoFe_2O_4$ bricklike nanoparticles, and (C) an annealed assembly of 8 nm/10 nm $FePt/CoFe_2O_4$ bricklike nanoparticles. Annealing was carried out at 700 °C under a reductive gas mixture (93% Ar + 7% H_2).

fcc to ordered $L1_0$ had begun at this temperature, as seen from the partial appearance of the FePt $L1_0$ superlattice peaks (Figure 4B). Further annealing of the bricklike particles at 600 and 700 °C resulted in a morphology change from bricklike particles to spherical particles (Figure 3C,D). The appearance of FePt $L1_0$ peaks in the XRD patterns showed that the chemically disordered fcc FePt particles had been transformed into a magnetically hard $L1_0$ phase (Figure 4C,D). Since the XRD patterns did not show any peaks other than those for the FePt $L1_0$ phase, HRTEM analysis was performed in order to characterize the phases formed in the nanocomposite material after annealing at 700 °C. HRTEM analysis (Figure 5A) and selected area electron diffraction (SAED) patterns (Figure 5B) revealed that two phases were present in the nanocomposite material, namely, the hard magnetic FePt $L1_0$ phase and the soft FeCo phase, which had diffused into each other to form polycrystalline nanocomposite particles with a spherical shape.

When the high-anisotropy $L1_0$ FePt phase developed after annealing at 700 °C for 2 h, a hard/soft FePt/FeCo exchange-coupled nanocomposite magnet was obtained. As shown in Figure 6, the coercivity (H_c) and saturation magnetization (M_s) of the annealed 8 nm/8 nm $FePt/CoFe_2O_4$ bricklike assembly were as high as 9.2 kOe and 926 emu/cm^3, respectively, as a result of exchange coupling, giving an energy product $(BH)_{max}$ of 15.5 MGOe. For comparison, the hysteresis loop of 8 nm $Fe_{46}Pt_{54}$ seeds annealed under similar conditions is also shown in Figure 6. One can see that the hysteresis loop of the 8 nm/8 nm nanocomposite particles shows smooth "single-phase" demagnetization behavior in the second quadrant with a high remanence ratio (M_r/M_s) of 0.73. Similar behavior was obtained for the nanocomposite $Fe_{58}Pt_{42}/Fe_3O_4$ binary systems.[10,12,16] This is typical behavior for an exchange-coupled nanocomposite magnet because of the interphase exchange coupling between the hard and soft phases.[17–19] The room-temperature hysteresis loop for the 8 nm/10 nm $FePt/CoFe_2O_4$ bricklike assembly annealed at 700 °C is also given in Figure 6. It was observed that with increasing soft-phase fraction, there was a decrease in coercivity and an increase in saturation magnetization of the nanocomposite, indicating that the energy product could be further improved by properly tuning the mass ratio of the two components. This suggests that the bricklike $FePt/CoFe_2O_4$ nanoparticles can indeed be used as building blocks to form nanocomposite magnets with enhanced magnetic performance.

Summary and Perspectives

In summary, this work has demonstrated that bimagnetic $FePt/CoFe_2O_4$ bricklike nanoparticles can be synthesized by growing $CoFe_2O_4$ on cubic FePt nanoparticle seeds. The size of the bricklike nanoparticles can be controlled by tuning the size of the $CoFe_2O_4$ components attached to the FePt nanoparticles. Reductive annealing transformed these bimagnetic bricklike nanoparticles into a hard magnetic nanocomposite with an enhanced energy product, indicating that the bimagnetic nanoparticles may serve as building blocks for high-performance permanent magnets and magnetic recording media. Independently altering the size of one or both of the components can enable the magnetic properties of these nanostructured systems to be tailored for further use in fabricating novel nanostructured magnetic devices. The major advantage of the bricklike morphology is that the surfaces of both components are available for further modifications, unlike a typical core/shell system where the surface of the core is completely covered by the shell. Our extended experiments show that with proper choice of materials (e.g., magnetic, semiconducting, optical), this synthetic procedure may be used to create bi-, tri-, or even tetra-component systems, which potentially can serve as versatile nanoplatforms for many desired applications.

Acknowledgment. This work was supported by ONR/MURI under Grant N00014-05-1-0497. We thank Dr. Guada Lian for the HRTEM analysis.

CM7028068

(16) Rong, C. B.; Nandwana, V.; Poudyal, N.; Li, Y.; Liu, J. P.; Ding, Y.; Wang, Z. L. *J. Phys. D: Appl. Phys.* **2007**, *40*, 712–716.
(17) O'Handley, R. C. *Modern Magnetic Materials: Principles and Applications*; John Wiley & Sons: New York, 2000; pp 437–514.
(18) Rong, C. B.; Zhang, H. W.; Chen, R. J.; He, S. L.; Shen, B. G. *J. Magn. Magn. Mater.* **2006**, *302*, 126–136.
(19) Rong, C. B.; Zhang, H. W.; Du, X. B.; Zhang, J.; Zhang, S. Y.; Shen, B. G. *J. Appl. Phys.* **2004**, *96*, 3921–3924.